FULL PAPER

Dalton
www.rsc.org/dalton

Enantioselectivity in Ni(II) Schiff-base complexes derived from amino-acids and (*S*)-*o*-*N*-(*N*-benzylprolyl)aminobenzophenone. Molecular structure of several chiral Ni(II) Schiff-base complexes, circular dichroism and molecular mechanics studies†

J. Costa Pessoa,*[a] I. Correia,[a] A. Galvão,[a] A. Gameiro,[a,c] V. Felix[b] and E. Fiuza[a]

[a] *Centro Química Estrutural, Departamento de Engenharia Química, Instituto Superior Técnico, Av. Rovisco Pais, 1049-001, Lisboa, Portugal*

[b] *Departamento de Química, CICECO, Universidade de Aveiro, 3810-193, Aveiro, Portugal*

[c] *Now at Cambridge Institute for Medical Reseach, Department of Clinical Biochemistry, Wellcome Trust/MRC, Building Addenbrooke's Hospital, Hills Road, Cambridge, UK CB2 2XY*

Received 15th March 2005, Accepted 10th May 2005
First published as an Advance Article on the web 24th May 2005

Several Ni(II) complexes derived from (*S*)-*o*-*N*-(*N*-benzylprolyl)aminobenzophenone ((*S*)-BBP) and amino acids of general formula [Ni((*S*)-BBP-L-(or D-)-aa)] were prepared. The crystal and molecular structures of [Ni((*S*)-BBP-Gly)], [Ni((*S*)-BBP-L-Ser)] and [Ni((*S*)-BBP-L-aaIm)] (aaIm = L-2-amino-3-(imidazol-1-yl)propanoate were determined by X-ray diffraction analysis. In the three complexes the nickel atoms display a square-planar coordination and the overall structure around the metal indicates that the entire Schiff-base ligands form quite rigid frameworks. Molecular mechanics calculations were carried out for complexes [Ni((*S*)-BBP-Gly)], [Ni((*S*)-BBP-Ser)] and [Ni((*S*)-BBP-aaIm)] containing either the L- or D-amino acid forms, and the factors controlling the stereoselectivity are discussed. Several other [Ni((*S*)-BBP-L-aa)] complexes are also prepared and their circular dichroism spectra in solution and of the solids dispersed in KBr disks are measured and discussed. In agreement with other studies in solution with similar [Ni((*S*)-BBP-aa)] complexes, the Cotton effects for the bands with λ_{max} at 520–530 nm are positive when the amino acids have the L-configuration at the α-carbon. The same is observed in this work for the solid-state CD spectra of all compounds.

Introduction

The importance of obtaining optically pure materials hardly requires restatement and the production of these compounds continues to be a growing area in industry[1] and research.[2] α-Amino acids are important compounds in virtually all disciplines of biology, medicine, biochemistry and chemistry, and are finding increasing utility in the synthesis of pharmaceuticals, agricultural products, the food industry and materials science. Optically pure proteinogenic amino acids are important commodities,[3,4] the methods for their synthesis being well established, mostly involving biotechnological processes, which directly yield optically pure products. Methods for the synthesis of optically pure non-proteinogenic amino acids, a field where enzymatic and microbiological methods are much more difficult to develop, have received much attention, namely for pharmaceutical applications or to be used for the control of plant growth and plant diseases, and for the production of new tailor-made peptides and enzyme inhibitors.[4–9] The utility of non-proteinogenic α-amino acids for the purpose of inducing novel conformational features and protease resistance to synthetic polypeptides also continues to be one of the rapidly developing areas of research.[5,10,11]

Because of the diverse nature of their side-chains there is a great variety of potential uses of homochiral-amino acids, and many different strategies for their asymmetric synthesis have been developed[4–7,12] Belokon and coworkers[13–15] extensively developed a set of quite useful methods, many of them based on reactions at the α- and β-carbon atoms of Cu(II) and Ni(II) complexes of amino acids and Schiff bases of (*S*)-*o*-*N*-(*N*-benzylprolyl)aminobenzophenone ((*S*)-BBP) **1**. The reaction of glycine with Ni(II) ions and (*S*)-BBP yields complex **2** (see Scheme 1). The possibilities offered by this chiral reagent were intensively investigated and reviewed by Belokon,[16–18] and despite the progress in the catalytic asymmetric synthesis of α-amino acids, this and related systems continue to be active fields of research.[11,19–26] The reactions performed normally yield products with the general formula **3**, which corresponds to the diastereoisomeric complexes [Ni((*S*)-BBP-L-aa)] and [Ni((*S*)-BBP-D-aa)] containing L- and D-amino acids, respectively. The L- and D-configurations often correspond to the (*S*)- and (*R*)-notations. However, as for some α-amino acids, *e.g.* sulfur-containing amino acids such as cysteine, the L- and D-correspond to (*R*)- and (*S*)-notations, respectively, we will use here the designations L- and D- for the amino acid residues in the present set of compounds. Thermodynamic equilibrium is often established between the diastereoisomers during the reactions and normally the one containing the L-amino acid is thermodynamically favoured. The yields and diastereoselectivities are generally high. The diastereoisomeric complexes can be separated by chromatography in stereochemically pure form, and easily hydrolysed to the free amino acids.

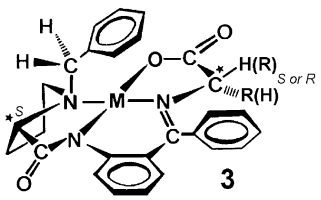

3

† Electronic supplementary information (ESI) available: Table SI–1: Deviations of coordinating atoms O(2), N(1), N(2), N(3) from the best least squared plane in complexes. Fig. SI–1: Conformations of rings A–C in complexes. Fig. SI–2: Relative positions of atoms in the coordination plane of complexes. See http://www.rsc.org/suppdata/dt/b5/b503786g/

DOI: 10.1039/b503786g

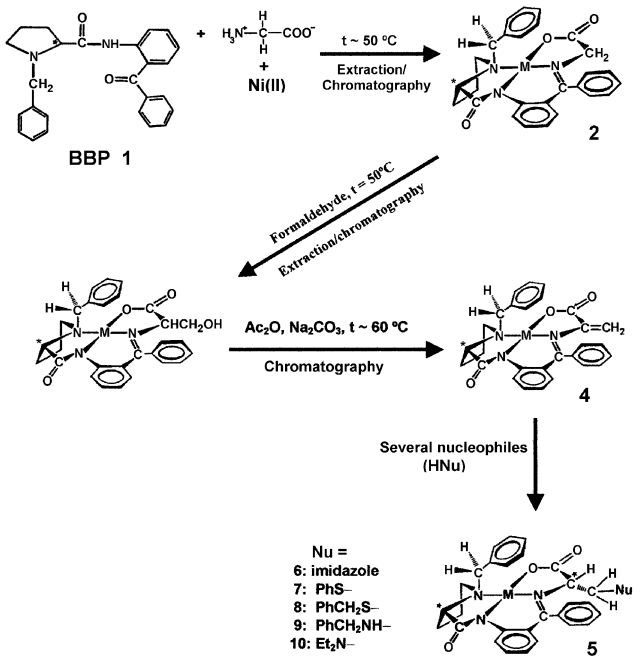

Scheme 1 Preparation of square-planar Ni(II) complexes **2–10**. By reaction of **2** with formaldehyde, a mixture of [Ni((*S*)-BBP-L-Ser)] and [Ni((*S*)-BBP-D-Ser)] is obtained; compound **11** corresponds to [Ni((*S*)-BBP-L-Ser)] and may be obtained from this mixture after chromatography (on a SiO_2 column). The several [Ni((*S*)-BBP-L-aa)] compounds **5** normally form in much higher amount than their [Ni((*S*)-BBP-D-aa)] isomers. Complexes **6–10**, containing the Schiff-base complexes of the L-amino acids, are obtained in a pure form after chromatography to separate the diastereoisomeric complexes.

In a related study,[27] the dehydroalanine intermediate **4** was prepared. The double bond of the dehydroalanine fragment is activated towards nucleophilic attack and this proved to be a reactive Michael acceptor for a variety of nucleophiles. The thermodynamically favoured *anti*-isomers **5** are formed and can be hydrolysed to produce the free amino acids, often with enantiomeric excess greater than 90%.

In the present work we report the crystal and molecular structure of the Ni(II) complexes **2** and [Ni((*S*)-BBP-L-Ser)], as well as of complex [Ni((*S*)-BBP-L-aaIm)] **6**, obtained on the reaction of **4** with imidazole. We also report the solid state and solution circular dichroism (CD) spectra of these and several other complexes obtained in similar reactions of **4** involving PhSH (**5**, Nu = –SPh) **7**, $PhCH_2SH$ (**5**, Nu = $–SCH_2Ph$) **8**, $PhCH_2NH_2$ (**5**, Nu = $–NHCH_2Ph$) **9** and Et_2NH (**5**, Nu = $–NEt_2$) **10**. Some molecular mechanics calculations are also presented for complexes [Ni((*S*)-BBP-Gly)], [Ni((*S*)-BBP-L-Ser)], [Ni((*S*)-BBP-D-Ser)], [Ni((*S*)-BBP-L-aaIm)] and [Ni((*S*)-BBP-D-aaIm)] to help sorting out the reasons for the stereoselectivity and CD spectra obtained.

Results and discussion

The molecular structures of complexes **2**, **6** and **11** are represented in Fig. 1. In all complexes the nickel presents a square-planar coordination geometry with small pyramidal distortions. Table 1 includes a selection of bond distances and angles, as well as some stereochemical data. Electronic supplementary information (ESI†) includes additional data, namely the deviations of the Ni–O(2)–N(1)–N(2)–N(3) atoms from the best planes defined by these atoms in complexes **2**, **6** and **11**. Globally the molecular structures of these complexes agree well with those determined for other similar/related compounds, *e.g.* [Ni((*S*)-BBP-L-3-*tert*-butyl-Ser)],[19] [Ni((*S*)-BBP-3FMeThr)] {(*S*)-BBP-3FMeThr = (Schiff base of (*S*)-BBP with (2*S*,3*S*)-2-(trifluoromethyl)threonine},[11] [Ni((*S*)-BAP-L-Ser)] {BAP = (*S*)-2-[*N*-(benzylprolyl)amino]acetophenone},[28]

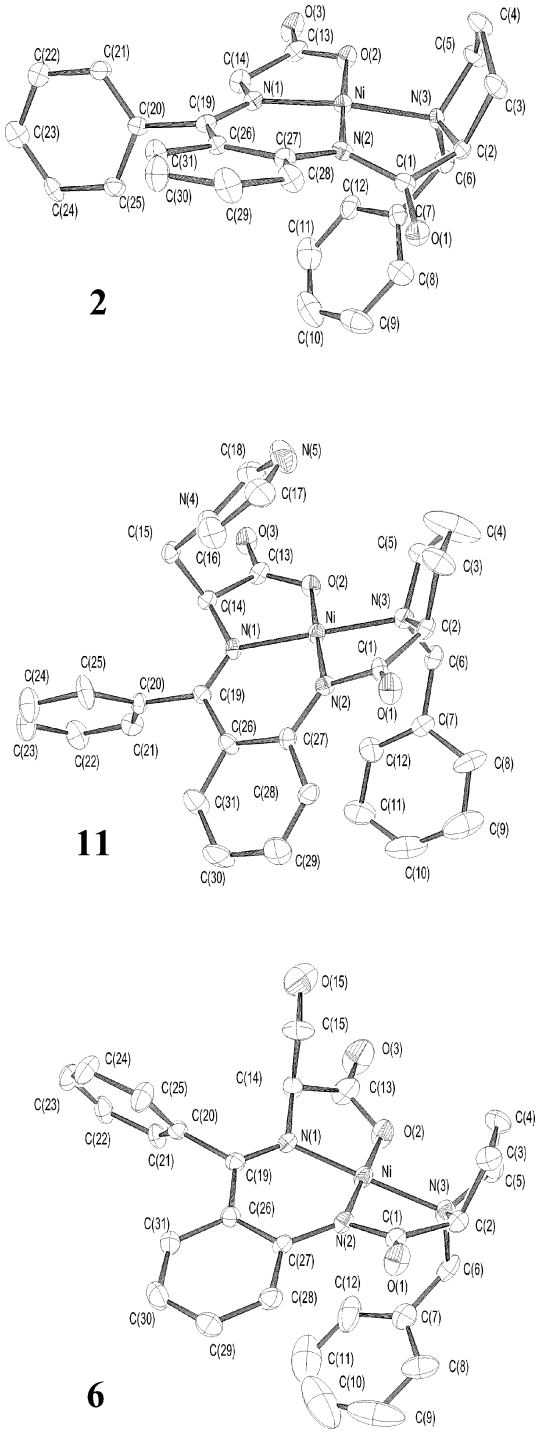

Fig. 1 ORTEP diagrams of [Ni((*S*)-BBP-Gly)] **2**, [Ni((*S*)-BBP-L-aaIm)] **6**, [Ni((*S*)-BBP-L-Ser)] **11**, with thermal ellipsoids at 20% probability. The atomic notation is indicated and similar numbering will be used throughout this work. The H atoms were omitted for clarity. For **6** the co-crystallization imidazole molecule present was also omitted. For **11** only one of the two possible positions of the L-serine side group is included.

[Ni((*S*)-BAP-D-Val)],[29] [Ni((*S*)-BAP-D-Val)],[15] and [Ni((*S*)-BBP-(2*S*,4*R*)-4-methyl glutamate)].[30]

We designate the three chelate rings of complexes [Ni((*S*)-BBP-aa)] by A, B, C. The five-membered ring A is defined by atoms NiO(2)C(13)C(14)N(1), the six-membered ring B is defined by atoms NiN(1)C(19)C(26)C(27)N(2) and the five-membered ring C is defined by atoms NiN(2)C(1)C(2)N(3). The chiral proline fragment induces chiral distortions on these chelate rings. Each of the rings has a particular conformation, and these are indicated in Table 1. Fig. SI–1 in the ESI† shows the conformations of the rings in complexes **2**, **6** and **11**. The

Table 1 Selected bond distances (Å), angles (°) and some structural and stereochemical data

		[Ni((*S*)-BBP-Gly)] **2**	[Ni((*S*)-BBP-L-Ser)] **11**	[Ni((*S*)-BBP-L-aaIm)][a] **6**
Square-planar centre	Ni–N(1)	1.862(6)	1.834(6)	1.874(9)
	Ni–N(2)	1.854(6)	1.845(6)	1.859(9)
	Ni–N(3)	1.945(5)	1.938(7)	1.933(11)
	Ni–O(2)	1.853(6)	1.869(6)	1.872(8)
	N(1)–Ni–N(2)	95.1(3)	93.9(3)	94.6(4)
	N(2)–Ni–N(3)	89.0(3)	87.0(4)	87.1(4)
	N(3)–Ni–O(2)	89.3(3)	92.7(4)	91.6(4)
	O(2)–Ni–N(1)	87.2(3)	86.4(4)	86.6(4)
	rms deviations from plane	0.100[b]	0.010[b]	0.008[b]
Ring A	Ni–O(2)–C(13)	116.5(5)	113.2(8)	114.9(8)
	C(14)–C(13)–O(2)	113.8(7)	114.8(8)	115.9(9)
	C(13)–C(14)–N(1)	110.1(7)	109.1(7)	106.7(10)
Deviations from plane of NiN(3)N(2)[c]	C(14)	+0.37	−0.54	−0.56
	C(13)	+0.19	−0.30	−0.35
		Asymmetric δ-envelope	Asymmetric λ-envelope	Asymmetric λ-envelope
Ring B	C(19)–N(1)–Ni	129.0(5)	128.0(6)	128.3(9)
	N(1)–C(19)–C(26)	121.2(8)	121.3(7)	120.3(11)
	C(19)–C(26)–C(27)	124.6(8)	124.4(7)	125.1(12)
	C(27)–N(2)–Ni	125.4(5)	125.1(5)	124.4(8)
Deviations from plane of NiN(1)N(2)[c]	C(19)	−0.02	0.38	0.39
	C(26)	−0.33	0.77	0.80
	C(27)	−0.33	0.53	055
		Asymmetric λ boat	Asymmetric δ boat	Asymmetric δ boat
Ring C	Ni–N(2)–C(1)	113.9(5)	113.1(5)	111.2(8)
	N(2)–C(1)–C(2)	112.5(7)	113.7(7)	115.8(11)
	C(2)–N(3)–Ni	106.4(4)	104.0(5)	106.8(8)
	N(2)–C(1)–O(1)	127.5(8)	126.8(8)	123.5(12)
	C(1)–C(2)–N(3)	112.2(6)	110.2(7)	111.4(11)
	Ni–N(3)–C(6)	107.2(5)	110.6(6)	107.7(9)
Deviations from plane of NiN(3)N(2)[c]	C(1)	+0.16	−0.53	−0.50
	C(2)	−0.20	−0.60	−0.76
		Symmetric λ skew	Asymmetric λ envelope	Asymmetric λ envelope

[a] The imidazolyl-centroid–Ni–benzyl centroid angle is 161°. [b] Root mean squares (rms) deviation of the coordinated atoms from the best plane formed by atoms Ni–N(1)–N(2)–N(3)–O(2). [c] The deviations are considered positive when the atom is on the same side as the benzyl group [atoms C(6)–C(12)].

distances of the atoms of the rings from the plane defined by the metal and the two coordinated atoms are also specified in Table 1 and in Fig. SI–1 [a positive value is given when the atom is on the side of the benzyl group, *i.e.* atoms C(6)–C(12)].

The conformations of each of the chelate rings A, B, C are similar for **6** and **11**, but differ for **2**. In complexes **6** and **11** the five-membered chelate rings A and C adopt an asymmetrical λ-envelope conformation; in **2** rings A and C correspond to an asymmetrical δ-envelope and symmetrical λ-skew conformations, respectively (for nomenclature see ref. 31, pp. 9–13). The six-membered chelate rings B of **6** and **11** adopt asymmetric δ boat conformations, but that of **2** an asymmetric λ boat conformation. This reflects the more relaxed structure of **2** as compared to **6** and **11** (see below). For each of the three complexes Table 1 includes the deviations of the carbon atoms of the chelate rings from the planes defined by the Ni and the corresponding two coordinated atoms. The benzyl group [atoms C(6)–C(12), C(6) bonded to N(3)] adopts distinct relative positions. This and the presence of the amino acid side groups in **6** and **11** and of the chiral proline fragment globally explain their different conformations and stereochemical features from those of **2**.

Previous investigations of the reactions of **2** with carbonyl compounds and the asymmetric synthesis of several β-substituted-α-amino acids by reaction of **4** with several nucleophiles defined many of the key parameters of reactivity of **2** and **4**, and origin of selectivity,[19,28,32] and two main types of diastereoselectivity were considered: one has its origin in the relative rates of *Re*- and *Si*-face addition, and the other is a thermodynamic control of the ratio of the two diastereomers formed. In some cases (*e.g.* [Ni((*S*)-BBP-Ser)])[28] it was observed that an equilibrium between diastereomers is established and the position of this equilibrium and the rate of epimerisation depends on pH.

Overall, the origin of the enantioselectivity observed in the formation of complexes [Ni((*S*)-BBP-L-aaIm)] and {[Ni((*S*)-BBP-L-Ser)] comes from the fact that for these isomers the benzyl group and the amino acid side-group lie on opposite sides of the coordination plane, while they are in the same side in their isomers [Ni((*S*)-BBP-D-aaIm)] and {[Ni((*S*)-BBP-D-Ser)]. The preference for the formation of the L-amino acids may also be due to the unfavourable intramolecular interactions of the amino acid side-chains with the phenyl substituent at the C(19)=N(1) bond, expected to be important for [Ni((*S*)-BBP-D-aa)], where these two groups are on the same side in relation to the Ni coordination plane, and not important for [Ni((*S*)-BBP-L-aa)]. However, for [Ni((*S*)-BBP-D-aa)] complexes to avoid such contacts the chelate rings may change their conformation, bond angles and torsions, and/or the benzyl, phenyl or amino acid side groups may rotate, and the final energy differences may be relatively small. For *e.g.* [Ni((*S*)-BAP-L-Val)] and [Ni((*S*)-BAP-D-Val)] it was estimated by MM calculations as 2.5 kJ mol^{-1}, and the barrier to rotation

of the benzyl group around the N(3)–C(6) bond was estimated not to exceed 21 kJ mol^{-1} for the same molecules.[29]

In order to better understand the stereoselective effects in the formation of the several complexes molecular mechanics (MM) calculations were carried out using the Universal Force Field (UFF),[33] within the CERIUS2 software.[34]

MM calculations can shed some light on the thermodynamics of the stereoselective effects, but it must be emphasized that our and previous MM calculations apply to the gas-phase structures, *i.e.*, entropic contributions, solvation, ion-pairing, intermolecular H-bonding and electrostatic effects were not taken into account, as is often done for coordination compounds.[35,36] Therefore, the calculations do not give definite answers and what follows should be considered in this light. Notwithstanding the MM calculations give structures that are free from the influence of crystal packing effects and other intermolecular interactions that may determine some features of the molecular structure of the complexes in the solid state. The MM calculated structures may therefore give better predictions of some solution spectroscopic data than those obtained from the X-ray data.

MM calculations were carried out for complexes [Ni((*S*)-BBP-Gly)], [Ni((*S*)-BBP-L-aaIm)], [Ni((*S*)-BBP-D-aaIm)], [Ni((*S*)-BBP-L-Ser)], [Ni((*S*)-BBP-D-Ser)]. Fig. 2 includes schematic representations of some of the MM structures of these compounds. The calculated energy differences ΔE(aaIm) = E{[Ni((*S*)-BBP-D-aaIm)] − E[Ni((*S*)-BBP-L-aaIm)]} = 41.8 kJ mol^{-1} and ΔE(Ser) = E{[Ni((*S*)-BBP-D-Ser)] − E[Ni((*S*)-BBP-L-Ser)]} = 32.6 kJ mol^{-1}, this being in agreement with the higher stability for the [Ni((*S*)-BBP-L-aa)] complexes. These values are significantly higher than those previously estimated for the [Ni((*S*)-BAP-aa)] complexes,[29] this being a reasonable result as in BBP there is one phenyl group instead of the methyl group present in BAP. However, the differences are higher than those expected from the diastereomeric ratios found in the synthetic procedures, where entropic contributions, solvation, *etc.* may be important.

The type of conformation of the chelate rings for the calculated MM structures for **2**, **6** and **11** is similar to those of the corresponding X-ray structures, except for ring C of **2** where a (slightly) asymmetric λ envelope was obtained instead of a symmetric λ skew (see ESI† for details). For almost all chelate rings the deviations of the carbon atoms from the planes formed by the Ni and two donor atoms are higher in the MM structures, this revealing a tendency in the MM structures to relax the strain around the Ni atom. In the crystals it is possible that this is constrained by the packing of the molecules. The differences between the bond distances and bond angles found in the X-ray and MM structures are relatively small, between 0–0.03 Å and 0–5°, (0–0.03 Å and 0–5°), being of the same order of the differences found within the X-ray structures of **2**, **6** and **11**. The differences of the torsion angles are greater (0–10°).

An evaluation of steric effects derived from the orientation (position) of the benzyl group in complexes **2**, **6** and **11** was made by progressively varying the torsion angle Ni–N(3)–C(6)–C(7). The phenyl group was rotated and the torsion angle constrained to specific values using a large force constant of 4184 kJ mol^{-1} rad^{-2}. With this constraint set at each value of the torsion angle Ni–N(3)–C(6)–C(7), the structure was then optimised using the CERIUS2 software. The energy profile found is shown in Fig. 3,

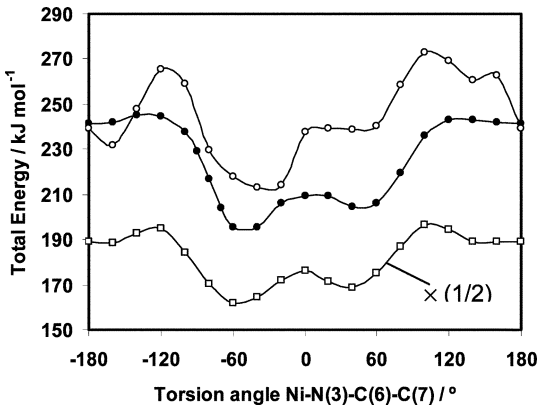

Fig. 3 Plot of the steric MM energy profile for [Ni((*S*)-BBP-Gly)] (●), [Ni((*S*)-BBP-L-aaIm)] (□, *E* values multiplied by 0.5) and [Ni((*S*)-BBP-L-Ser)] (○), calculated by constraining the torsion angle Ni–N(3)–C(6)–C(7) at specific values, which defines the position of the benzyl group.

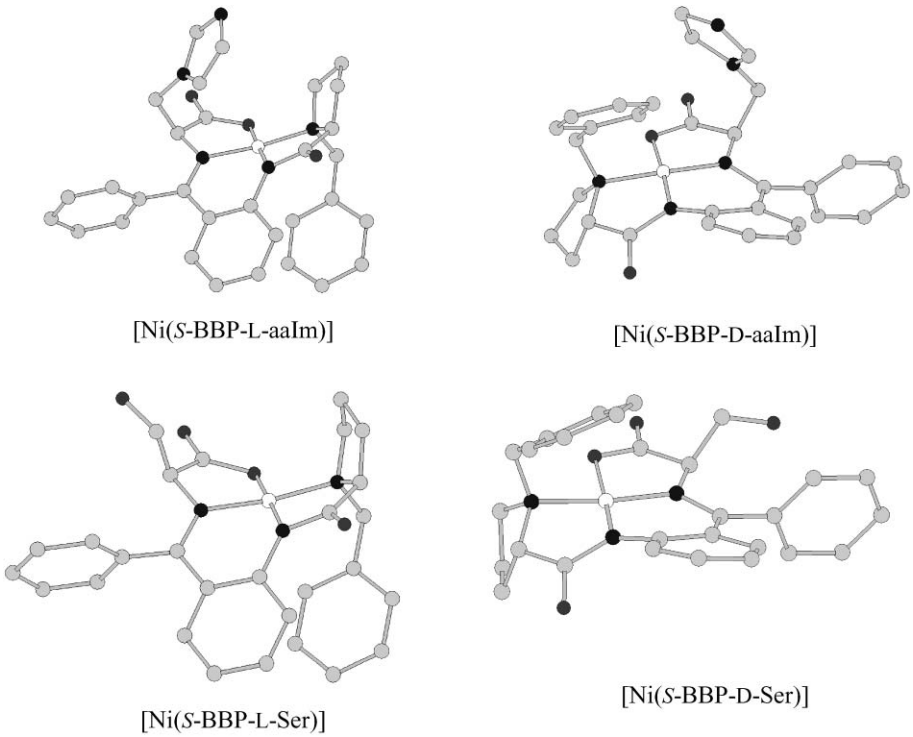

Fig. 2 Molecular mechanics optimised structures of [Ni((*S*)-BBP-L-aaIm)], [Ni((*S*)-BBP-D-aaIm)] and of [Ni((*S*)-BBP-L-Ser)], [Ni((*S*)-BBP-D-Ser)].

showing two main energy minima for complexes **2** and **6** (at *ca.* −60 and −40°), and one for **11** at *ca.* −35/−45° (with a plateau between *ca.* 0 and 60°). The global barrier for total rotation of the benzyl group ($E_{max} - E_{min}$) are *ca.* 58, 63 and 50 kJ mol^{-1} for **2**, **6** and **11**, respectively. The main terms contributing to the calculated energies with CERIUS2 as the torsion angles Ni–N(3)–C(6)–C(7) are varied are the angle and van der Waals terms, followed by the torsion term. As the size of the amino acid side group increases the van der Waals term becomes more important (see Table 2).

The torsion angles Ni–N(3)–C(6)–C(7) in the structures determined by X-ray are −41.0, −57.9 and −56.6° for **2**, **6** and **11**, respectively. These do not correspond exactly to the minimum energy structures as calculated by MM, but the calculated energies for these and the X-ray structures only differ by less than *ca.* 8.4 kJ mol^{-1}. There are some intramolecular close contacts in the X-ray structures that do not exist or are relaxed in the MM optimised structures and some others that persist. In a few rare cases some contacts are closer in the MM structures (see Table 3). The MM calculated structures for the [Ni((*S*)-BBP-D-aaIm)] and [Ni((*S*)-BBP-D-Ser)] globally show closer contact distances than those of the [Ni((*S*)-BBP-L-aaIm)] and [Ni((*S*)-BBP-L-Ser)], and globally the several groups of the ligands (benzyl, prolyl, phenyl and amino acid side group) are closer. This is reflected in the higher values of the angle, torsion and van der Waals energy terms shown in Table 2 for [Ni((*S*)-BBP-D-aaIm)] and [Ni((*S*)-BBP-D-Ser)]. Overall, each of the several groups of [Ni((*S*)-BBP-aaIm)] and [Ni((*S*)-BBP-Ser)] are rigidly fixed by the framework of the macrocyclic complex molecule and cannot change their position much. If this happens, normally either new intramolecular contacts appear, or the existing ones become closer. Complexes [Ni((*S*)-BBP-D-aaIm)] and [Ni((*S*)-BBP-D-Ser)] are particularly constrained and globally their higher energy as compared to [Ni((*S*)-BBP-L-aaIm)] and [Ni((*S*)-BBP-L-Ser)] is due mainly to angle, torsion and van der Waals energy terms (not mainly due to the van der Waals term alone). Observation of the deviations of the Ni-O(2)–N(1)–N(2)–N(3) atoms from the best planes, calculated for the X-ray and MM structures, give significantly lower values for [Ni((*S*)-BBP-aaIm)] and [Ni((*S*)-BBP-Ser)] (L- or D-amino acids) than for [Ni((*S*)-BBP-Gly)] (see Fig. SI–2 in ESI†), this being the result of the latter complex possessing a less rigid structure.

In the electronic spectra of square-planar Ni(II) complexes, theory predicts[37] that three or four transitions, depending on the symmetry of the complex and on the π-acid–base properties of the ligands,[38] should occur within the d-orbital manifold of the metal ion. For the present compounds two bands are recorded in the 400–700 nm range, one at 420–460, and a second broad one with λ_{max} at 520–530 nm. Circular dichroism spectra can often resolve a broad absorption band into several components; for example, Nishida and Kida[39] studied the d–d spectra of some square-planar Cu(II) and Ni(II) quadridentate amides and Schiff-base complexes and found that three distinct CD bands are observable in the 400–670 nm region, whereas in the isotropic absorption spectra normally only one band was observed in this region. Fig. 4 shows CD spectra in CH_2Cl_2 of several complexes with general formula **5**, and Table 4 some λ_{max} data. In is interesting to note that in the CD spectrum of **4** (not shown), band I is as intense as that of **8**. The pattern of the spectra is similar in all cases. Three distinct CD bands are normally observable in the 400–650 nm region (four for the L-serine derivative, shown in Fig. 5) with a (−),(−),(+) pattern, while normally two are recorded for the corresponding isotropic electronic spectra. Judging from the intensity of the broad VIS bands at 520–530 nm (<300), they should be mainly due to d–d transitions. The nature of the absorption observed at 420–460 nm is more difficult to assess. In some cases it appears as a shoulder on the low-energy side of much more intense charge-transfer and imine n→π* bands at $\lambda < 420$ nm and probably also include the magnetic dipole-allowed $d_{xy} \rightarrow d_{x^2-y^2}$ transition (band III).

Depending on the π-basicity of the ligand the relative energies of the d_{xy} and d_{xz},d_{yz} bands may vary.[37,38] The lower-energy VIS absorption band at 520–530 nm certainly has the same origin as that of the observed lower-energy CD band, and we will

Table 2 Energy (kJ mol^{-1}) of the several energy terms upon changing the torsion angle Ni–N(3)–C(6)–C(7)[a] (see text and Fig. 3)

	Minimum of energy term	Value of energy term for the optimised structure (or see[b])	Maximum of energy term	$E_{max} - E_{min}$
[Ni((*S*)-BBP-Gly)]		[b] −30.7°		
Bonds	17.0	17.0	23.0	5.9
Angles	71.2	79.7	107.3	36.1
Torsions	97.1	99.0	110.8	13.8
Inversions	0.54	0.54	1.1	0.58
van der Waals	16.1	16.8	34.0	17.9
Total	213.1	213.1	272.5	59.4
[Ni((*S*)-BBP-aaIm)]		[b] L-isomer: −54.3° [b] D-isomer: −65.4°		
Bonds	15.2	L-: 15.2, D-: 23.4	21.8	6.6
Angles	224.0	L-: 224.0, D-: 230.1	259.6	10.7
Torsions	101.0	L-: 104.6, D-: 107.8	108.3	7.3
Inversions	1.3	L-: 1.8, D-: 0.54	2.0	0.63
van der Waals	−23.8	L-: −23.8, D-: 1.6	6.9	30.8
Total	321.8	[b] L-: 321.8, D-: 363.5	392.3	64.1
[Ni((*S*)-BBP-Ser)]		[b] L-isomer: −50.4°, [b] D-isomer: −48.2°		
Bonds	15.3	L-: 15.3, D-: 23.1	19.4	4.1
Angles	77.0	L-: 78.3, D-: 82.0	110.2	33.2
Torsions	98.4	L-: 102.6, D-: 109.7	103.3	4.9
Inversions	0.8	L-: 1.2, D-: 0	1.4	0.54
van der Waals	−6.1	L-: −4.6, D-: 10.4	19.2	25.3
Total	192.9	L-: 192.9, D-: 225.6	244.8	49.5

[a] Most values given for **6** and **11** are for the [Ni((*S*)-BBP-L-aa] diastereomers. Only for the globally optimised structures (3rd column) the energy terms are specified for the [Ni((*S*)-BBP-L-aa] and [Ni((*S*)-BBP-D-aa] diastereomers. [b] The torsion angle Ni–N(3)–C(6)–C(7) for the globally optimised structure of the diastereomers: [Ni((*S*)-BBP-L-aa] (L-isomer) and [Ni((*S*)-BBP-D-aa] (D-isomer) are given.

Table 3 Close contacts (in Å) found in the X-ray structures of **2**, **6** and **11** and in the MM optimised structures of [Ni(BBP-Gly)], [Ni(BBP-(L- or D-)-aaIm)] and [Ni(BBP-(L- or D-)-Ser)][a,b]

X-Ray structure	MM optimised structure	MM optimised structure	MM optimised structure
[Ni(BBP-Gly)]	[Ni(BBP-Gly)]		
C(20) *2.44* H–C(31)	{C(20) *2.67* H–C(31)}		
O(2) *2.39* H–C(5)	O(2) *2.51* H–C(5)		
O(1) *2.21* H–C(28)	O(1) *2.43* H–C(28)		
[Ni(BBP-L-aaIm)]	[Ni(BBP-L-aaIm)]	[Ni(BBP-D-aaIm)]	[Ni(BBP-D-aaIm)]
O(1) *2.28* H–C(28)	O(1) *2.43* H–C(28)	O(2) *2.46* H–C(5)	C(8) *2.72* H–C(5)
O(2) *2.33* H–C(5)	O(2) *2.47* H–C(5)	O(1) *2.48* H–C(28)	{N(5) *2.95* H–C(9)}
C(20) *2.49* H–C(14)	{C(20) *2.80* H–C(14)}	C(25) *2.56* H–C(15)	C(31) *2.54* H–C(21)
C(20) *2.46* H–C(31)	C(20) *2.65* H–C(31)	C(20) *2.72* H–C(31)	C(21) *2.63* H–C(14)
C(20) *2.86* C(31)	C(20) *3.00* C(31)	C(20) *3.06* C(31)	
Ni *2.69* H–C(12)	Ni *2.40* H–C(12)	Ni *2.19* H–C(12)	{C(21)–H *2.37* H–C(8)}
Ni *3.10* C(12)	Ni *2.90* C(12)	Ni *3.03* C(12)	
[Ni(BBP-L-Ser)]	[Ni(BBP-L-Ser)]	[Ni(BBP-D-Ser)]	[Ni(BBP-D-Ser)]
O(2) *2.29* H–C(5)	O(2) *2.28* H–C(5)	O(2) *2.26* H–C(5)	
O(3) *2.19* H–O(4)	O(1) *2.43* H–C(28)	O(1) *2.46* H–C(28)	
O(1) *2.22* H–C(28)	{C(13) *3.00* H–O(4)}	C(8) *3.23* N(2)	
C(13) *2.49* H–O(4)	{O(3) *2.89* H–O(4)}	C(6)–H *2.28* H–C(2)	
Ni *3.24* C(12)	Ni *2.93* C(12)	Ni *2.87* C(12)	
Ni *3.20* C(7)	Ni *3.07* C(7)	Ni *2.84* C(7)	Ni *2.87* C(12)
C(6) *3.08* N(2)	C(6) *3.49* N(2)	C(6) *3.46* N(2)	Ni *2.55* H–C(12)
C(7) *3.10* N(2)	C(7) *3.21* N(2)	C(7) *3.02* N(2)	C(12) *3.23* N(2)
C(20) *2.84* C(31)	C(20) *3.01* C(31)	C(20) *3.02* C(31)	
C(20) *2.44* H–C(31)	C(20) *2.66* H–C(31)	C(20) *2.68* H–C(31)	
C(20) *2.49* H–C(14)	C(20) *2.70* H–C(14)	C(11) *3.18* H–C(9)	
C(20) *2.82* C(14)	C(20) *3.07* C(14)	C(20) *3.02* C(14)	

[a] The numbers included between atoms correspond to the internuclear distances in Å. [b] When { ··· } is used, this means that the distance is relatively short, not below the sum of the van der Waals radius, but it corresponds to a relevant stereochemical feature.

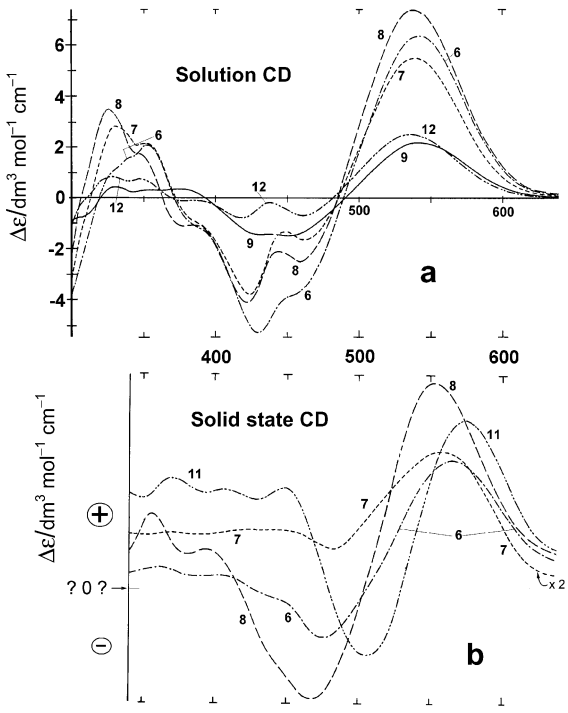

Fig. 4 CD spectra of solutions of Ni((*S*)-BBP-aa complexes. (a) in dichloromethane. (b) CD spectra of solid samples of the same Ni((*S*)-BBP-aa) complexes dispersed in KBr disks. In (b), the signal obtained for **7** is multiplied by 2. In most cases, the CD signal is noisy in the range 400–450 nm (400–500 nm for **7**) and the spectra shown are not entirely reliable in this range. With this type of solid sample, one does not know the position of the base line ($\Delta\varepsilon = 0$), and this may differ for the several spectra shown. Therefore, the line included is just a rough indication of its possible position.

consider here that it corresponds to the $d_{xy} \rightarrow d_{x^2-y^2}$ transition (band I).[37,40] This transition has a relatively large rotatory strength as expected for a magnetic dipole-allowed d–d transition. The bands at 420–440 nm and at ≈475 nm have a weaker intensity. They have contributions from transitions originating at the d_{z^2} (magnetic dipole-forbidden),[40] and d_{xz},d_{yz}, which may originate magnetic dipole-allowed d–d transitions.[40]

Fig. 5 includes CD spectra of [Ni((*S*)-BBP-Gly)], [Ni((*S*)-BBP-L-Ser)] and [Ni((*S*)-BBP-D-Ser)] in CH_2Cl_2 solution and in the solid state (samples dispersed in KBr disks). As for the spectra of the compounds included in Fig. 4, for all complexes the CD solid state spectrum resembles the corresponding CD solution spectrum, indicating that the main factors that determine the CD spectra are the same, *e.g.* the conformations, torsions and atom positions relatively to the Ni and coordinated atoms. The only exception is [Ni((*S*)-BBP-Gly)] and the differences found in this case are discussed below.

Belokon and coworkers, *e.g.* refs.[14,15,32] found that the sign of the Cotton effect in the 500–600 nm region (band I) was always positive for complexes containing L-amino acids and negative for those containing D-amino acids. This general trend was not influenced by the structure of the α-amino acid's side-chain. This is the case for all spectra in Fig. 4, for the dehydroalanine derivative **4**, and also for **2**, compounds **2** and **4** not containing a dissymmetric carbon in the amino acid fragment. Belokon and coworkers[27] also presented ORD curves for compounds **6–9** and our results are consistent with these ORD curves; however in CD spectra the bands are sharper, and although they also overlap rather strongly, approximate λ_{max} values can be extracted from the spectra and similarities become more apparent. In the solid state the CD spectra of band I is also positive for complexes containing L-amino acids (*e.g.* Figs. 4 and 5).

One should emphasize that overlapping, oppositely signed CD bands tend to cancel and change the real positions of the λ_{max}

Table 4 Circular dichroism data for CH_2Cl_2 solutions of Ni((*S*)-BBP-aa) complexes[a]

Complex	λ_{max}/nm ($\Delta\varepsilon$/dm^3 mol^{-1} cm^{-1})
2	240 (+3.8); 280 (−4.7); 325 (+3.1); 350 (+4.3); 427 (−7.8); 525 (+5.7)
4	330 (+3.4); 350 (+2.1); 385 (+0.4); 425 (−2.8); 462 (−1.95); 540 (+7.2)
6	332 (+1.2); 355 (+2.1); ~385 (−1.2); 430 (−5.3); ~460 (−3.8); 543 (+6.3)
7	330 (+2.8); 355 (+2.2); 385 (−1.1); 425 (−3.8); 462(−1.7); 540 (+5.3)
8	325 (+3.5); 350 (+1.8); 380 (−1.3); 422 (−4.2); 463 (−2.3); 538 (+7.4)
9	330(+0.4)[b]; ~352(+0.2)[b]; ~375(+0.3)[b]; ~430(−1.3)[b]; ~455(−1.4)[b]; 543(+2.0)
10	312 (−2.2); 338 (−0.2); 375 (+1.8); 447(−3.35); 550 (+2.5)
11	327 (+3.2); 350 (+1.9); 375 (−0.37); 418 (−0.94); 435 (+1.1); 462 (−1.1); 535 (+7.0)
11A[c]	305 (−3.8); 325 (−1.7); 370 (+3.1); 422 (+5.8); 445(+3.4); 545 (−2.9)
12[c]	330 (+0.9); 350 (+0.75); 380 (−0.15); 420 (−0.8); 460 (−0.7); 537 (+2.5)

[a] The bands in the range 535–545 correspond to band I (see text). The bands at 445–465 and 420–435 nm may have contributions from bands II and III, respectively, and from other transitions (see text). [b] The spectrum is noisy; the values presented are only approximate. [c] **11A**: Ni((*S*)-BBP-D-Ser); **12**: Ni((*S*)-BBP-L-Thr).

values. Therefore the values in Table 4 are only approximations of the correct λ_{max}. Fig. 5 includes the CD and UV-VIS spectra of complexes [Ni((*S*)-BBP-Gly)], [Ni((*S*)-BBP-L-Ser)] and [Ni((*S*)-BBP-D-Ser)]. The CD of band I does indeed become negative for [Ni((*S*)-BBP-D-Ser)], however, as some other CD bands do not change sign, the CD bands add up with a final totally distinct appearance in the UV range, although they mostly show opposite signs in the visible range, namely for band I.

The global CD signal in metal complexes may be considered as resulting from the sum of several effects:[41] (i) inherent dissymmetry, (ii) configurational, (iii) vicinal, (iv) conformational and (v) donor atom distortions [the order of importance is normally (i) > (ii) > (iii) > (iv); the relative importance of effect (v) varies with the donor atom distortions and may be the strongest]. Belokon and coworkers, *e.g.* refs. 15 and 42 discussed the intensities of the CD bands of the [Ni((*S*)-BBP-aa)] complexes in the 400–600 nm range as due to what they designate as the vicinal contributions [effect (iii)] of the ligand. Strictly this should mean that the CD intensity is transmitted through space from the asymmetric atom to the chromophore by way of the chemical bonds linking the asymmetric centre to the chromophore.[41] This will depend on the nature, size and distance of the amino acid side chain to the Ni centre. For other square-planar Ni(II) complexes other authors have considered the conformational effect (iv) to be the determining factor (*i.e.*, it is the conformation of the chelate rings that determine the type of CD spectra obtained),[43,44] or that the main origin of CD strength comes from the asymmetric arrangement of the donor atoms and/or asymmetric deviation of the donor atoms from a regular symmetrical polyhedron [effect (v)].[45–47]

The plane of the donor atoms is a nodal surface for generation of optical activity[48] and all atoms that do not belong to this nodal plane and are disposed in an asymmetric fashion around the Ni(II) atom may contribute to the CD signal. This means that for the present set of complexes any effect (iii)–(v) may contribute to the CD strength. In the ESI† we include several schematic representations of the distortions from the average coordination plane for the X-ray and MM structures. Due to the global steric requirements these distortions from the average coordination plane are higher for [Ni((*S*)-BBP-Gly)] than for the [Ni((*S*)-BBP-(D or L)-Ser)] and [Ni((*S*)-BBP-(D or L)-aaIm)] complexes. Moreover, the type of atom displacements from the plane of all atoms of each chelate ring is the same for all MM calculated structures (which we consider as a good approximation for the solution structures), but differs from the X-Ray structures of [Ni((*S*)-BBP-L-Ser)] and [Ni((*S*)-BBP-L-aaIm)]. Nevertheless, the type of CD spectra recorded, namely the $\Delta\varepsilon$ values for band I are always the same: $\Delta\varepsilon$(band I) > 0 for the [Ni((*S*)-BBP-L-aa)] complexes, as well as **2** and **4**, and $\Delta\varepsilon$(band I) < 0 for the [Ni((*S*)-BBP-D-aa)] complexes. This implies that for complexes [Ni((*S*)-BBP-L-Ser)] and [Ni((*S*)-BBP-L-aaIm)] effect (v) is not determining the CD signal, and that it should be the conformational and/or the vicinal effects that determine the signal and intensity of the CD in the visible range.

When a side chain is introduced into the amino acid residue, the equilibrium between conformations of the several chelate rings shifts towards the one that corresponds to less strain and electronic repulsions. In Fig. SI–1 (ESI†) it may be seen that the type of conformation of rings A, B and C in the X-ray and MM structures is the same {for ring C of [Ni((*S*)-BBP-Gly)] see discussion below}, but for each ring the atom deviations from the planes of Ni and the two donor atoms increase in the order: Gly < Ser < aaIm, *i.e.*, increase with the bulkiness of the amino acid side chain. This also means that for each ring the interconversions between conformations certainly becomes more difficult as the size of the side chain increases, *i.e.* the conformational effect also increases. In Fig. 4 it may be seen that there is no clear relation between the intensities of the CD signals in the visible range, namely band I, and the bulkiness of the amino acid side group. Therefore, although both the contributions of chelate ring conformations and of the vicinal effect may operate, the vicinal effect cannot explain by itself the differences in CD signal intensities.

A factor that may also be important is borrowing of CD intensity from charge transfer. However, comparing the X-ray and MM calculated structures no relation was found between the relative positions and distances between the groups that may possibly contribute and the stereogenic centers, so we could not establish any relation between the structural details and the CD spectra obtained.

The point that remains to be explained are the opposite signals of band I in the CD spectra of [Ni((*S*)-BBP-Gly)] in solution and in the solid state. In complex [Ni((*S*)-BBP-Gly)], there is no vicinal effect due to an amino acid side chain, both the X-ray and MM structures present significant atom deviations from the best coordinating plane, but the type and size of deviations are very similar. The only relevant differences are: (i) for ring B the distances of the C(19) atom from the plane of N(1), Ni, N(2) (0.02 Å in the X-ray and 0.22 Å in the MM structure), and (ii) for ring C the conformations differ (symmetric λ skew in the X-ray, and slightly asymmetric λ envelope in the MM structure). These differences may explain the CD spectra shown in Fig. 5(a), assuming that the MM structure is an adequate representation of [Ni((*S*)-BBP-Gly)] in CH_2Cl_2 solution.

Experimental

Preparations

All reagents were obtained from commercial sources. All reactions were monitored by TLC on Merck silica gel 60 TLC plates (Art. 5626, 20 × 10). IR spectra were recorded on a BioRad FTS 3000 MX FTIR spectrometer and ^{1}H NMR with a Varian Unity 300 Spectrometer at room temperature.

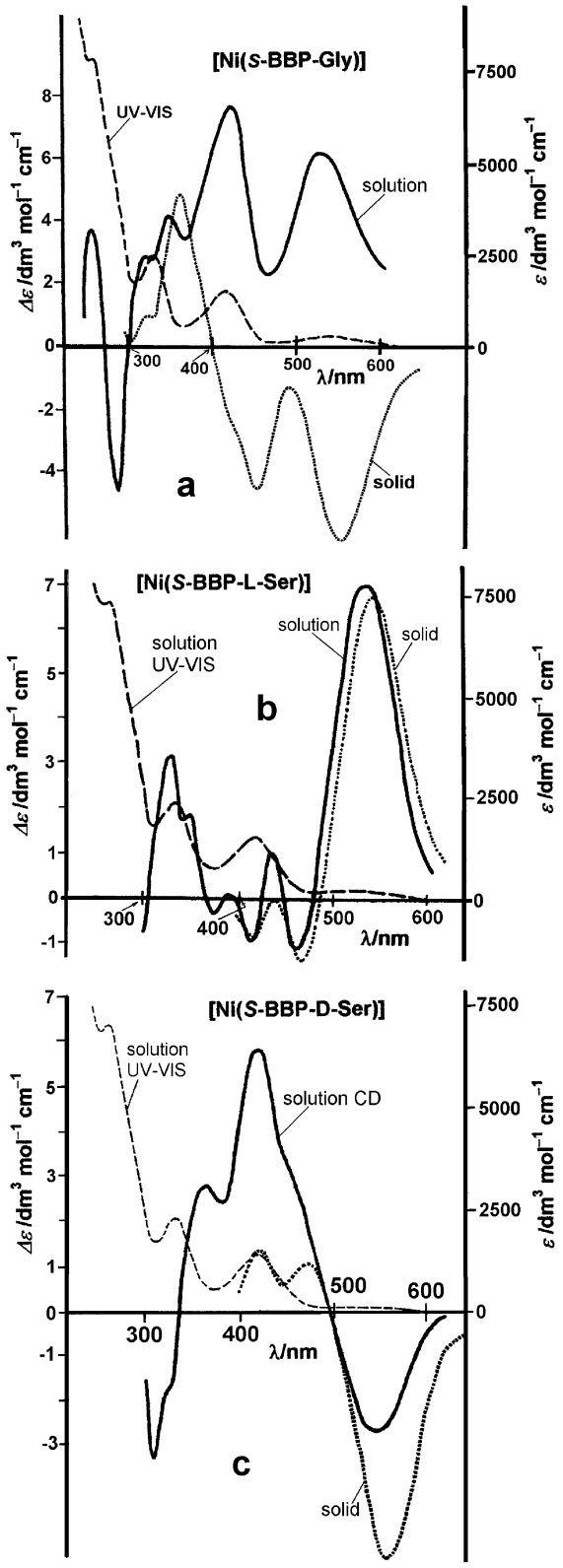

Fig. 5 UV-Vis and CD spectra of (a) [Ni((*S*)-BBP-Gly)], (b) [Ni((*S*)-BBP-L-Ser)] and (c) [Ni((*S*)-BBP-D-Ser)] in CH_2Cl_2 solution and CD spectra in the solid state (samples dispersed in KBr disks).

Complex **2** was obtained as previously described[28] and this was converted to the corresponding serine complex (**3**; R = $-CH_2OH$) **11**, *via* MeONa catalysed condensation with formaldehyde.[28] This was dehydrated by the action of Ac_2O in MeCN, to produce **4**, also as previously described.[27] The products were purified by chromatography on silica columns and were characterized by elemental analysis, IR, CD and ^{1}H NMR spectra. Here and below the ^{1}H NMR spectra obtained agree with those previously reported for the same compounds.

Condensations of complex **4** with imidazole, Et_2NH, $PhCH_2NH_2$, PhSH and $PhCH_2SH$ and separation of products were conducted similarly to the procedures described in ref. 27 The compounds were characterized by elemental analysis, IR, CD and ^{1}H NMR spectra. In particular, the condensation of **4** with imidazole yielded a mixture, which was filtered, and the filtrate and washings evaporated under reduced pressure. The residue recrystallised from benzene–acetone (6 : 1) yielded **6**. On slow evaporation of the mother liquor, crystals of **6** suitable for X-ray were obtained. Crystals of **2** were obtained from slow evaporation of a CH_2Cl_2 solution of the compound and crystals of **3** from slow evaporation of one of the fractions collected in the chromatographic separation of the [Ni((*S*)-BBP-L-Ser)] and [Ni((*S*)-BBP-D-Ser)] diastereoisomeric complexes.

Circular dichroism and isotropic absorption spectra

UV-VIS spectra were recorded either on a Hitachi U-2000 or on a Perkin-Elmer Lambda 9 UV/VIS/NIR spectrophotometer. CD spectra were run on a JASCO 720 spectropolarimeter either using the UV-VIS (200–700 nm) or the VIS (400–1000 nm) photomultiplier.

Solid samples for CD spectra. For each solid an extremely fine powder containing KBr was ground (agate mortar) and a disk prepared. This was placed between two microscope slides in the sample compartment in a fixed position. A first CD spectrum was run, the sample rotated 60–80° and another spectrum recorded; at least five rotations were performed for each sample and the corresponding spectrum recorded. With this type of solid sample, one does not know the position of the base line but the correct pattern may be obtained if the spectrum recorded after each rotation of the sample is always approximately the same. The final CD spectrum taken for each compound is the average of the several CD spectra recorded for that compound. Samples dispersed in Nujol mulls were also prepared and their CD spectra recorded as described in ref. 49, the CD spectra obtained normally being very similar to those of the KBr disks.

Crystallography

X-Ray data were collected at room temperature from crystals of complexes **2**, **6** and **11** mounted in thin-walled glass capillaries. Data were collected at room temperature on Enraf-Nonius MACH3 diffractometer with graphite-monochromatized Mo-Kα radiation (λ = 0.71069 Å), using an ω–2θ scan mode. Unit cell dimensions were obtained by least-squares refinement of the setting angles of 25 reflections. The crystal data are summarized in Table 5. The data were corrected[50] for Lorentz-polarization effects, for linear decay and empirically for absorption. The heavy atom positions were located by Patterson methods using SHELXS 86.[51] The remaining atoms were located in successive Fourier-difference maps and refined by least squares on F^2 using SHELXL 97.[52] In **11** the oxygen atom labelled O15 was found to be disordered over two positions labelled O15A and O15B. The occupancy values were refined as free variables, and the occupancies found were 0.60(2) and 0.40(2), respectively.

In the structure of **6** a co-crystallization imidazole molecule was also located in the Fourier-difference map, which precluded a good quality structural refinement. This solvation molecule was refined with the constraint of being a regular pentagon. All the non-hydrogen atoms were refined with anisotropic thermal motion parameters. The hydrogen atoms were included in calculated positions (except the 4 hydrogen atoms of the co-crystallization imidazole molecule), constrained to ride at fixed distances of the parent atom. The Flack X parameter, calculated without using Friedel reflections in the refinement, may be considered ~0.0 for all compounds, but the values in the CIF files are −0.10(4), 0.03(6) and −0.01(4) for compounds **2,6** and **11**, respectively. Atomic scattering factors and anomalous

Table 5 Crystallographic data for complexes **2**, **6** and **11**

	2	**6**	**11**
Formula	$C_{27}H_{25}N_3NiO_3$	$C_{34}H_{29}N_7NiO_3$ [a]	$C_{28}H_{27}N_3NiO_4$
M	498.26	646.4	528.29
Crystal system	Orthorhombic	Orthorhombic	Orthorhombic
Space group	$P2_12_12_1$	$P2_12_12_1$	$P2_12_12_1$
a/Å	9.044(1)	10.875(1)	9.564(2)
b/Å	9.722(1)	12.042(2)	10.115(1)
c/Å	26.445(5)	24.834(3)	25.500(7)
U/Å^3	2325	3252	2467
Z	4	4	4
D_c/g cm^{-3}	1.42	1.31	1.41
μ(Mo-Kα)/mm^{-1}	0.869	0.641	0.827
F(000)	1040	1336	1092
No. refl. measured	2921	4411	2519
No. unique refl. (R_{sigma})	2888 (0.077)	4381 (0.12)	2493 (0.036)
$R1$ ($I > 2\sigma(I)$)	0.06	0.11	0.05
$wR2$	0.12	0.29	0.16

[a] The number of hydrogen atoms is 33, but the four hydrogen atoms of the co-crystallization imidazole molecule were not included in the refinement.

dispersion terms were as in SHELXL 97.[52] The ORTEP drawings were made with ORTEP-3.[53] WINGX[54] was used as interface for all programs.

CCDC reference numbers 266340–266342.

See http://www.rsc.org/suppdata/dt/b5/b503786g/ for crystallographic data in CIF or other electronic format.

Molecular mechanics calculations

Molecular mechanics calculations were carried out using the Universal Force Field (UFF),[33] within the CERIUS2 software.[34] This force field is parameterised for full periodic, but the minimization of a few X-ray structures revealed clearly that the default parameters found in the field were inappropriate to reproduce accurately the coordination spheres of the complexes. Therefore a specific set of parameters comprising the L–M bond lengths and L–M–L angles was developed empirically in order to reproduce the coordination spheres found for **2**, **6** and **11**. Partial charges were not included as they were difficult to calculate accurately and only have marginal impact on relative strain energies in metal complexes. All model complexes were minimised using the conjugate gradient algorithm and a high convergence criteria with default parameters.

Conclusions

Several Ni(II) complexes derived from the reaction of (*S*)-BBP **1** and amino acids of general formula [Ni((*S*)-BBP-L-(or D)-aa)] were prepared and the crystal and molecular structures of [Ni((*S*)-BBP-Gly)], [Ni((*S*)-BBP-L-Ser)] and [Ni((*S*)-BBP-L-aaIm)] were determined by X-ray diffraction analysis. In each of the three complexes the Ni atoms has a square-planar coordination and the overall structure corresponds to a quite rigid framework, particularly [Ni((*S*)-BBP-L-Ser)] and [Ni((*S*)-BBP-L-aaIm)]. The molecular mechanics calculations also indicate that in this type of molecule the several groups present (phenyl, benzyl, prolyl and amino acid side groups) must assume rather rigid positions, determined by a complex balance of close contacts, bond distances and bond angles. When the amino acids have the D-configuration at the α-carbon, this balance is not easily accomplished and the structures correspond to a significantly higher steric energy. At least for [Ni((*S*)-BBP-Ser)] and [Ni((*S*)-BBP-aaIm)] this determines the stereoselectivity found in the preferred formation of the amino acids with L-configuration.

Concerning the CD spectra of the several complexes prepared, as the coordinating atoms do not deviate much from the best plane formed by these and Ni, these deviations cannot originate significant contributions to the CD signal. Moreover, the correlation between the size of the amino acid side group and the CD signal intensities in the visible range is not good. Our results indicate that although the vicinal effect may have a significant contribution, the conformational effect has at least a similar but probably more important contribution to the CD signals.

As observed for the CD solution spectra, in the CD solid state spectra the Cotton effects for band I are positive when the amino acids have the L-configuration at the α-carbon. Moreover, for most complexes the type of CD spectra recorded in the solid state and in solution are similar, which indicates that the main factors that determine these spectra are the same, *i.e.*, the structures are very similar in both media. Complex [Ni((*S*)-BBP-Gly)] has a less rigid structure that the other compounds studied. The differences found between the CD spectra of [Ni((*S*)-BBP-Gly)] in solution and in the solid state probably arise from the possibility that some of the chelate rings of [Ni((*S*)-BBP-Gly)] have different conformations in the two media, as indicated by the comparison of the X-ray and MM structures.

Acknowledgements

We would like to thank Fundação para a Ciência e Tecnologia (FCT), POCTI (POCTI/QUI/ 55985/2004), and Fundo Europeu para o Desenvolvimento Regional (FEDER) for financial support. We also thank Paula Rosa and Adelaide Sousa for the preparation of some compounds.

References

1 S. C. Stinson, *Chem. Eng. News*, 1994, **38**, 38.
2 *Chem. Rev.*, 2003, **103** (ed. C. Bolm and J. A. Gladysz).
3 *Chirality in Industry. The Commercial Manufacture and Applications of Optically Active Compounds*, ed. A. N. Collins, G. N. Sheldrake and J. Crosby, John Wiley & Sons, Chichester, 1992.
4 R. M. Williams, *Synthesis of Optically Active a-Amino Acids*, Pergamon, Oxford, 1989.
5 R. O. Duthaler, *Tetrahedron*, 1994, **50**, 1539–1650.
6 C. Cativiela and M. D. Días-se-Villegas, *Tetrahedron: Asymmetry*, 1998, **9**, 3517–3599.
7 F. P. J. T. Rutjes, L. B. Wolf and H. E. Schoemaker, *J. Chem. Soc., Perkin Trans. 1*, 2000, 4197–4212.
8 R. M. Williams, *Chem. Rev.*, 1992, **92**, 889.
9 D. Seebach, A. R. Sting and M. Hoffman, *Angew. Chem., Int. Ed. Engl.*, 1996, **35**, 2708.
10 A. Spatola, *Chemistry and Biochemistry of Amino acids, Peptides and Proteins*, Marcel Decker, New York, 1983, p. 267.
11 V. A. Soloshonok, V. P. Kukhar, S. V. Galushko, N. Yu Svistunova, D. V. Avilov, N. A. Kuz'mina, N. I. Raevski, Yu. T. Struchkov, A. P. Pysarevsky and Yu. N. Belokon, *J. Chem. Soc., Perkin Trans. 1*, 1993, 3143–3155.

12 K. Maruoka and T. Ooi, *Chem. Rev.*, 2003, **103**, 3013–3028.
13 Yu. N. Belokon, I. E. Zel'tzer, M. G. Ryzhov, M. B. Saporovskaya, V. I. Bakhmutov and V. M. Belikov, *J. Chem. Soc., Chem. Commun.*, 1982, 180–181.
14 Yu. N. Belokon, I. E. Zel'tzer, V. I. Bakhmutov, M. B. Saporovskaya, M. G. Ryzhov, A. I. Yanovsky, Yu. T. Struchkov and V. M. Belikov, *J. Am. Chem. Soc.*, 1983, **105**, 2010–2017.
15 Yu. N. Belokon, V. I. Maleyev, S. V. Vitt, M. G. Ryzhov, Yu. D. Kondrashov, S. N. Golubev, Yu. P. Vauchskii, A. I. Kazika, M. I. Novikova, P. A. Krasutskii, A. G. Yurchenko, I. L. Dubchak, V. E. Shklover, Yu. T. Struchkov, V. I. Bakhmutov and V. M. Belikov, *J. Chem Soc., Dalton Trans.*, 1985, 17–26.
16 Yu. N. Belokon, *Pure Appl. Chem.*, 1992, **64**, 1917–1924.
17 Yu. N. Belokon, *Bull. Russ. Acad. Sci.*, 1993, **41**, 868–884.
18 M. G. Ryzhov and Yu. N. Belokon, *Russ. J. Appl. Chem.*, 1994, **67**, 101–104.
19 V. A. Soloshonok, D. V. Avilov, V. P. Kukhar, V. I. Taravorov, T. F. Savel'eva, T. D. Churkina, N. S. Ikonnikov, K. A. Kochetkov, S. A. Orlova, A. P. Pysarevsky, Yu. T. Struchkov, N. I. Raevski and Yu. N. Belokon, *Tetrahedron: Asymmetry*, 1995, **6**, 1741–1756.
20 J. Jirman and A. Popkov, *Collect. Czech. Chem. Commun.*, 1995, **60**, 990–998.
21 Yu. N. Belokon, N. B. Bespalova, T. D. Churkina, I. Cisarová, M. G. Ezernitskaya, S. R. Harutyunyan, R. Hrdidina, H. B. Kagan, P. Kocovsky, K. A. Kochetkov, O. V. Larionov, K. A. Lyssenko, M. North, M. Polásek, A. S. Peregudov, V. V. Prisyazhnyuk and S. Vyskocil, *J. Am. Chem. Soc.*, 2003, **125**, 12860–12871.
22 A. S. Saghiyan, A. V. Geolchanyan, S. M. Djamgaryan, S. M. Vardapetyan, V. I. Tararov, N. A. Kuz'mina, N. S. Ikonnikov, Yu. N. Belokon and M. North, *Russ. Chem. Bull., Int. Ed.*, 2000, **49**, 1460–1463.
23 A. S. Saghiyan, A. V. Geolchanyan, L. L. Manasyan, G. M. Mkrtchyan, N. R. Martirosyan, S. A. Dadayan, T. V. Kochickyan, S. R. Harutyunyan, A. A. Avetisyan, V. I. Tararov, V. Maleev and Yu. N. Belokon, *Russ. Chem. Bull., Int. Ed.*, 2004, **53**, 932–935.
24 A. S. Saghiyan, A. V. Geolchanyan, S. G. Petrosyan, T. V. Ghochikyan, V. S. Haroutunyan, A. A. Avetisyan, Yu. N. Belokon and K. Fisher, *Tetrahedron: Asymmetry*, 2004, **15**, 705–711.
25 R. N. Krasikova, V. V. Zaitsev, S. M. Ametamey, O. F. Kuznetsova, O. S. Fedorova, I. K. Mosevich, Yu. N. Belokon, S. Vyskocil, S. V. Shatik, M. Nader and P. A. Schubinger, *Nucl. Med. Biol.*, 2004, **31**, 597–603.
26 Yu. N. Belokon, S. R. Harutyunyan, E. V. Vorontsov, A. S. Peregudov, V. N. Chrustalev, K. A. Kochetkov, D. Pripadchev, A. S. Sagyan, A. K. Beck and D. Seebach, *ARKIVOC*, 2004, **iii**, 132–150.
27 Yu. N. Belokon, A. S. Sagyan, S. M. Djamgaryan, V. I. Bakhmutov and V. M. Belikov, *Tetrahedron*, 1988, **44**, 5507–5514.
28 Yu. N. Belokon, A. G. Bulychev, S. V. Vitt, Yu. T. Struchkov, A. S. Batsanov, T. V. Timofeeva, V. A. Tsyryapkin, M. G. Ryzhov, L. A. Lysova, V. I. Bakhmutov and V. M. Belikov, *J. Am. Chem. Soc.*, 1985, **107**, 4252–4259.
29 S. V. Lindeman, T. V. Timofeeva, V. I. Maleyev, Yu. N. Belokon, M. G. Ryzhov, V. M. Belikov and Yu. T. Struchkov, *Acta Crystallogr., Sect. C*, 1985, **41**, 1290–1295.
30 Yu. N. Belokon, A. G. Bulychev, M. G. Ryzhov, S. V. Vitt, A. S. Batsanov, Yu. T. Struchkov, V. I. Bakhmutov and V. M. Belikov, *J. Chem. Soc., Perkin Trans. 1*, 1986, 1865–1872.
31 C. J. Hawkins, *Absolute Configuration of Metal Complexes*; Wiley-Interscience, New York, 1971, pp. 8–15.
32 Yu. N. Belokon, A. S. Sagyan, A. A. Djamgaryan, V. I. Bakhmutov, S. V. Vitt, A. S. Batsanov, Yu. T. Struchkov and V. M. Belikov, *J. Chem. Soc., Perkin Trans. 1*, 1990, 2301–2310.
33 A. K. Rappé, C. J. Casewit, K. S. Colwell, W. A. Goddard, III and W. M. Skiff, *J. Am. Chem. Soc.*, 1992, **114**, 10024.
34 *CERIUS 2 (v3.5)*, San Diego, Molecular Simulations Inc., 1997.
35 P. Comba, *Coord. Chem. Rev.*, 1999, **182**, 343–371.
36 P. Comba and T. W. Hambley, *Molecular Modeling of Inorganic Compounds*, Wiley-VCH, Weinheim, 1995.
37 A. B. P. Lever, *Inorganic Electronic Spectroscopy*, Elsevier, Amsterdam, 1984, pp. 534–544.
38 Y. Nishida and S. Kida, *Coord. Chem. Rev.*, 1979, **27**, 275–298.
39 Y. Nishida and S. Kida, *Bull. Chem. Soc. Jpn.*, 1970, **43**, 3814.
40 B. J. Bosnich, *J. Am. Chem. Soc.*, 1968, **90**, 627–632.
41 R. Kuroda and Y. Saito, Circular Dichroism of Inorganic Complexes: Interpretation and Application, in *Circular Dichroism Principles and Applications*, ed. K. Nakanishi, N. Berova and R. W. Woody, VCH, New York, 1994, pp. 217-258.
42 Yu. N. Belokon, V. I. Bakhmutov, N. I. Chernoglazova, K. A. Kochetkov, S. V. Vitt, N. S. Garbalinskaya and V. M. Belikov, *J. Chem. Soc., Perkin Trans. 1*, 1988, 305–312.
43 J. P. Costes, J. M. Dominguez-Vera and J. P. Laurent, *Polyhedron*, 1995, **14**, 2179–2187.
44 R. S. Downing and F. L. Urbach, *J. Am. Chem. Soc.*, 1970, **92**, 5861–5865.
45 N. C. Payne, *Inorg. Chem.*, 1973, **12**, 1151–1156.
46 K. Okazaki and K. Saito, *Bull. Chem. Soc. Jpn.*, 1982, **55**, 785–791.
47 A. Wojtczak, E. Szlyk, M. Jaskóski and E. Larsen, *Acta Chem. Scand.*, 1997, **51**, 274–278.
48 J. W. Chang and R. B. Martin, *J. Phys. Chem.*, 1969, **73**, 4277–4283.
49 I. Cavaco, J. Costa Pessoa, D. Costa, M. T. L. Duarte, R. D. Gillard and P. M. Matias, *J. Chem. Soc., Dalton Trans.*, 1994, 149–157.
50 C. K. Fair, *MOLEN*, Enraf-Nonius, Delft, 1990.
51 G. M. Sheldrick, *SHELXS 86, Program for the Solution of Crystal Structure*, University of Gottingen, 1986.
52 G. M. Sheldrick, *SHELXL-97, Program for the Refinement of Crystal Structure (release 97-2)*, University of Gottingen, 1997.
53 L. J. Farrugia, Ortep-3 for Windows, *J. Appl. Crystallogr.*, 1997, **30**, 565.
54 L. J. Farrugia, WingX (v1.64.03b), *J. Appl. Crystallogr.*, 2002, **32**, 837–838.